

An Integrated Risk Assessment and Collision Avoidance Methodology for an Autonomous Catamaran with Fuzzy Weighting Functions

Pouria Sarhadi
School of Electronics, Electrical
Engineering and Computer Science
Queen's University Belfast
Belfast, UK
p.sarhadi@qub.ac.uk

Wasif Naeem
School of Electronics, Electrical
Engineering and Computer Science
Queen's University Belfast
Belfast, UK
w.naeem@qub.ac.uk

Nikolaos Athanasopoulos
School of Electronics, Electrical
Engineering and Computer Science
Queen's University Belfast
Belfast, UK
n.athanasopoulos@qub.ac.uk

Abstract— Collision avoidance and risk assessment are open problems to be practically addressed in maritime transportation. In high-speed vessels this problem becomes more challenging due to manoeuvring and reaction time constraints. Here, a reactive collision avoidance and risk assessment technique with fuzzy weighting functions are proposed for a relatively high-speed autonomous catamaran. To follow paths between predefined waypoints, a Line of Sight (LOS) technique with Cross Tracking Error (CTE) is utilised. Besides, a new collision risk index is introduced based on fuzzy weighting functions. To perform formal maritime decision making, the standard marine COLLISION REGULATIONS (COLREGs) are incorporated into the algorithm. Furthermore, a simplified Closest Point of Approach (CPA) formulation is presented. The proposed framework is simulated on a realistic model of a vessel including input and non-holonomic constraints and disturbances. Simulation results for various encounter scenarios demonstrate the merits of the proposed method.

Keywords—motion planning, collision avoidance, risk assessment, autonomous vessel, COLREGs

I. INTRODUCTION

Increasing the autonomy level in marine vessels has been gaining momentum over the last ten years with numerous papers written and many research and development projects funded [1-9]. Although the initial focus was on the military domain, civilian use has recently attracted significant interest to electrical, and self-propelled ferries being developed including the Yara Birkeland [5] in Norway and Artemis Hydrofoiling Ferry [6] in the UK. As part of the Belfast Maritime Consortium, zero-emissions ferries with an electric hydrofoil propulsion system are targeted in [6]. One of the ambitious aims of this project is vessel autonomy and the development of a captain assist system for collision prevention in dynamic environments. Safety remains one of the main challenges in all types of manned or unmanned vehicles. Therefore, presenting advanced safe motion planning techniques is of outstanding interest to relevant scientific and industrial communities. As the first step in this journey, the paper investigates the risk assessment and COLLISION AVOIDANCE (COLAV) problem of an autonomous vessel.

Crucial areas in local motion planning of autonomous vessels are path following, collision avoidance, COLREGs compliance, risk assessment and feasibility of implementation in real time. As mentioned, a plethora of research has been carried out in improving the autonomy of maritime vessels. For instance, in [10] velocity obstacles (VO) method with CPA calculations is deployed for avoiding hazards and

obeying COLREGs. In [11] Model Predictive Control (MPC) is applied to a similar COLAV problem with the simulated trajectories to anticipate the behaviour of the obstacles and ship instead of the CPA. Discrete and constrained versions of the Artificial Potential Fields (APFs) are proposed in [12] and [13], respectively. In [14], a Multiobjective Optimization Approach is proposed for the COLREGs-Compliant path planning and implemented on a ship bridge simulator. Moreover, different approaches for the risk analysis of the ship motion are presented in [15-18]. Recent techniques in this field are comprehensively reviewed in [2-4]. Each method has its pros and cons as surveyed in [2, 3] and exploring all of them is infeasible within the confines of this paper. The main contributions of the paper include: (1) proposing new nonlinear fuzzy weighting functions for the COLAV problem with dynamic obstacles; (2) developing a novel risk index; and (3) embedding COLREGs in the aforementioned algorithms. Last, (4) CPA calculations are reformulated to make the procedure simpler to understand and implement. Owing to the low computational burden of the proposed algorithm, it is suitable for real-time applications.

The rest of the paper is organised as follows. Section II presents the problem statement. The path planning, COLAV and control algorithms are discussed in Section III. The proposed risk assessment technique and COLREGs integration are explained in Section IV. Simulation results and analysis are presented in Section V and Section VI concludes the paper.

II. PROBLEM STATEMENT

In this research, a marine vessel navigates in open water with a goal to track predefined waypoints, in the presence of disturbances and (static or dynamic) obstacles. Motion planning and COLAV algorithms are applied to follow the waypoints while the obstacles are avoided. Risk analysis should be activated for each obstacle and when required, any evasive action should be COLREGs-compliant. Eventual exploitation of those algorithms would either be an autopilot, or a captain assist system for manned vessels. A schematic presentation of a typical scene and its related parameters are shown in Fig. 1. The importance of using a realistic model to assess path planning algorithms are discussed in [4]. In this paper, the following differential equations are utilised to model the vehicle motion:

$$\dot{X}(t) = u(t)\cos(\psi(t)) \quad (1)$$

$$\dot{Y}(t) = u(t)\sin(\psi(t)) \quad (2)$$

$$\dot{\psi}(t) = r(t) \quad (3)$$

$$\dot{r}(t) = -\left(\frac{1}{T_\psi}\right)r(t) + \left(\frac{1}{T_\psi}\right)K_\psi(\tau(t) - d(t)) \quad (4)$$

$$\dot{d}(t) = -\left(\frac{1}{T_d}\right)d(t) + \omega_d(t) \quad (5)$$

$$\dot{u}(t) = -\left(\frac{1}{T_u}\right)u(t) + \left(\frac{1}{T_u}\right)K_u u_c(t) \quad (6)$$

where $[X, Y, \psi]$ are the pose of the vessel to include the X and Y coordinates and heading angle, r is the yaw rate, u is the vessel speed, and d is the random disturbance modelled by a first order Markovian process with ω_d and T_d as its random input and time constant, respectively. The signal $d(t)$ models the wave drift forces, low-frequency wind and ocean currents [19]. The variable $\tau(t)$ accounts for the steering input to the vessel. An input amplitude saturation is also applied in all simulations to consider the vessel manoeuvring limitations such as minimum turning radius. K_ψ and T_ψ are the gain and time constants of the first order Nomoto yaw dynamics [19]. K_u and T_u are the gain and time constant to model the speed behaviour as a first-order system. The variable u_c stands for the vessel cruise controller reference which in this paper, it is set to a constant number. Overall, the above model considers the dynamics of the heading alongside the non-holonomic and actuation limitations as well as environmental disturbances. Hence, the proposed motion planning and control algorithms are evaluated here for realistic conditions. In the following, the procedure to design the algorithms is presented in further details.

III. PATH PLANNING, COLAV AND CONTROL ALGORITHMS

In this section, the integrated path planning, collision avoidance and control algorithms used in this paper are discussed. As mentioned earlier, a high-level mission planner is assumed to provide the desired waypoints to be followed by the vessel. The path planning algorithm generates the necessary yaw references to follow the waypoints, whilst the COLAV system alters this value on-the-fly to avoid any collision during a mission. Therefore, the overall yaw demand (ψ_d) consists of the waypoint-based LOS reference (ψ_{wp}) and additional demand for COLAV (ψ_{COLAV}) as given by (7):

$$\psi_d(t) = \psi_{wp}(t) + \psi_{COLAV}(t) \quad (7)$$

In addition, a Proportional Derivative (PD) controller with rate feedback is employed to steer the vessel to closely follow the path. The procedure to design those algorithms are described in the following sections.

A. Path Planning Algorithm

In the context of path planning, a LOS technique with CTE is adopted [20]. Each waypoint has its specified position as $WP(i) = [X_{wp(i)}, Y_{wp(i)}]$, and the LOS-CTE algorithm generates the required yaw demand (ψ_{wp}) to track the path between successive waypoints (Fig. 1). For a general i -th waypoint, the error signals in X and Y direction between the waypoint and the current position of the vessel $[X_{ewp(i)}, Y_{ewp(i)}]$ can first be defined as:

$$X_{ewp(i)}(t) = X_{wp(i)} - X(t) \quad (8)$$

$$Y_{ewp(i)}(t) = Y_{wp(i)} - Y(t) \quad (9)$$

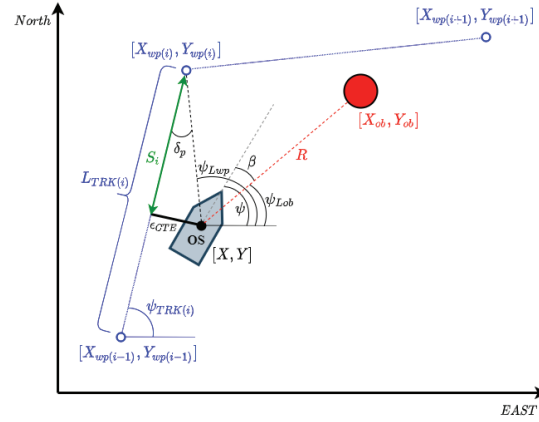


Fig. 1. Schematic figure of the vessel in path following and obstacle avoidance

Hence, the corresponding LOS angle can be computed by the following equation:

$$\psi_{LWP}(t) = \text{atan2}(Y_{ewp(i)}(t), X_{ewp(i)}(t)) \quad (10)$$

where atan2 returns the arctangent confined to $(-\pi, \pi]$. On the other hand, the track length ($L_{TRK(i)}$) and the track angle ($\psi_{TRK(i)}$) (see Fig.1) for the straight line between the i -th and the $(i-1)$ -th waypoints can be calculated by the following formulae:

$$L_{TRK(i)} = \sqrt{(X_{wp(i)} - X_{wp(i-1)})^2 + (Y_{wp(i)} - Y_{wp(i-1)})^2} \quad (11)$$

$$\psi_{TRK(i)} = \text{atan2}(Y_{wp(i)} - Y_{wp(i-1)}, X_{wp(i)} - X_{wp(i-1)}) \quad (12)$$

The distance to the i -th waypoint $S_i(t)$ projected on the track- proportional to the track length ($L_{TRK(i)}$) is:

$$S_i(t) = \frac{(X_{ewp(i)}(X_{wp(i)} - X_{wp(i-1)}) + Y_{ewp(i)}(Y_{wp(i)} - Y_{wp(i-1)}))}{L_{TRK(i)}} \quad (13)$$

Thus, the cross-track error ϵ_{CTE} in Fig. 1 can be computed as:

$$\epsilon_{CTE}(t) = S_i(t) \tan(\delta_p(t)) \quad (14)$$

where $\delta_p(t)$ is the difference between the track angle and LOS angle given by:

$$\delta_p(t) = \psi_{TRK(i)} - \psi_{LWP} \quad (15)$$

Subsequently, the waypoint yaw reference $\psi_{wp}(t)$ to keep the vessel on the track can be calculated as [20]:

$$\psi_{wp}(t) = \psi_{LWP}(t) - \text{atan}(\epsilon_{CTE}(t)/\mu) \quad (16)$$

where μ is a tuning parameter related to the vehicle's manoeuvrability. The logic to switch to the next waypoint is based on the distance to the current waypoint [19]. Hence, if $\sqrt{X_{ewp(i)}(t)^2 + Y_{ewp(i)}(t)^2} < D_m$ is satisfied, the algorithm switches to track the following waypoint ($(i+1)$ -th) provided by the mission planner, D_m being the radius of a circle of acceptance around each waypoint.

B. COLAV based on Fuzzy Weightings

The collision avoidance algorithm is an extension of a practical avoidance method proposed in [20] for Autonomous Underwater Vehicles (AUVs). Although the early version was developed for static obstacles, it is demonstrated in this paper that this method can also deal with dynamic obstacles. The

general concept is to allocate fuzzy weights to the distance and the bearing of each obstacle. Then the COLAV yaw demand (ψ_{COLAV}) can be computed using the product of the distance and bearing weighting functions. The fuzzy weighting function for the distance is considered as the following Z-shaped Membership Function (ZMF):

$$w_R(x, a, b) = ZMF(x, a, b) = \begin{cases} 1, & x < a \\ 1 - 2\left(\frac{(x-a)/(b-a)}{2}\right)^2, & a \leq x \leq (a+b)/2 \\ 2\left(\frac{(x-a)/(b-a)}{2}\right)^2, & (a+b)/2 \leq x \leq b \\ 0, & x > b \end{cases} \quad (17)$$

The shape of this function is shown in Fig. 2. The argument of this function in COLAV is the Euclidean distance (R) between a given obstacle and the own ship as in (18):

$$R(t) = \sqrt{(X_{ob}(t) - X(t))^2 + (Y_{ob}(t) - Y(t))^2} \quad (18)$$

Where $[X_{ob}, Y_{ob}]$ is the position vector of the given obstacle in the global frame. Therefore, based on Fig. 2(a), the range weighting increases when the distance is less than b and reaches its maximum value once the distance to the obstacle is closer than a . For the bearing angle to the obstacle, the following Gaussian function is exploited [20]:

$$w_\beta(x, \sigma) = e^{-\beta^2/2\sigma^2} \quad (19)$$

Where σ is the standard deviation of the Gaussian function and β is the bearing angle that can be calculated as follows:

$$\beta(t) = \psi(t) - \text{atan2}(Y_{ob}(t) - Y(t), X_{ob}(t) - X(t)) \quad (20)$$

Owing to the Gaussian property, when β is within $\pm 3\sigma$, this function applies a larger weight to the bearing as shown in Fig. 2(b). To enable the algorithm to select between the starboard or the port move, or stand-on the following form of (19) is introduced:

$$w_\beta(x, \sigma) = e^{-\beta^2/2\sigma^2} \quad (21)$$

Finally, the COLAV yaw command for each obstacle ($\psi_{COLAV(i)}$) can be determined as a product of both weights as follows:

$$\psi_{COLAV(i)} = K_{Dir} K_{COLAV(i)} w_{R(i)} w_{\beta(i)} \quad (22)$$

where K_{COLAV} is a tuning knob to select the amplitude of ψ_{COLAV} for each obstacle, and $K_{Dir} \in \{-1, 0, 1\}$ is a parameter to select the direction of the movement. Hence, the final COLAV action can be computed a the summation of COLAV commands for all obstacles.

C. Control technique

The control algorithm is a Proportional Derivative (PD) controller with rate feedback with following equation:

$$\tau(t) = K_p(\psi_{com}(t) - \psi(t)) - K_d r(t) \quad (23)$$

where τ is the steering input to the vessel. An amplitude input saturation is also applied in simulations to consider the physical limitations of the vessel.

IV. RISK ASSESSMENT AND DECISION MAKING BASED ON THE COLREGS

In this section, the risk assessment and COLREGs-based decision making are addressed.

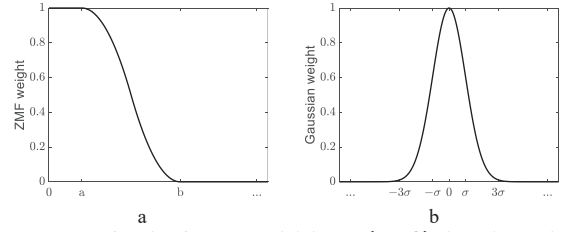


Fig. 2. a) ZMF function for range weighting $w_R(x, a, b)$, b) and Gaussian function for bearing weighting $w_\beta(x, \sigma)$

A. Risk Assessment

In maritime transportation, there are several techniques to calculate the risk of collision. However, the Closest Point of Approach (CPA) is the most widely accepted method in risk analysis [4, 21-22]. For this purpose, two main criteria, i.e. Distance to CPA (DCPA) and Time to CPA (TCPA) are commonly used [4, 21]. CPA calculations have been presented in the literature with different formulations [23-26]. Here a convenient method to translate maritime navigation fundamentals into a practical algorithm is presented [27]. A scene showing a Target Ship (TS) approaching the Own Ship (OS) is illustrated in Fig. 3. The CPA circle definition is based on the relative velocity vector V_{rel} between the Own Ship (OS) and the Target Ship (TS). The CPA point is the tangent to a circle fitted to the centre of the OS as the extension of V_{rel} vector (point A in Fig. 3); and two crucial DCPA and TCPA indexes are to predict the distance and the time to collide at the CPA point. If DCPA ≈ 0 and the TCPA decreases over time, a collision is being anticipated. The following geometrical equations can calculate those two indexes as follows:

$$DCPA(t) = R(t) \sin(\alpha(t)) \quad (24)$$

$$TCPA(t) = R(t) \cos(\alpha(t)) / V_{rel}(t) \quad (25)$$

To handle the above equations, the relative velocity (V_{rel}) and its angle ($\psi_{V_{rel}}$) can be computed by:

$$V_{rel}(t) = \sqrt{(V_{xob}(t) - V_x(t))^2 + (V_{yob}(t) - V_y(t))^2} \quad (26)$$

$$\psi_{V_{rel}}(t) = \text{atan2}(V_{yob}(t) - V_y(t), V_{xob}(t) - V_x(t)) \quad (27)$$

where $[V_x(t), V_y(t)]$ and $[V_{xob}(t), V_{yob}(t)]$ are the velocity vectors of the OS and any obstacle (or the TS) at time t . If the reciprocal angle between the OS and the obstacle is given as:

$$\rho(t) = \text{atan2}(Y(t) - Y_{yob}(t), X(t) - X_{yob}(t)) \quad (28)$$

by considering Fig. 3, the α angle between $\psi_{V_{rel}}$ and ρ can be computed by: $\alpha(t) = \rho(t) - \psi_{V_{rel}}(t)$, so,

DCPA/TCPA can be easily computed using (24-25).

As mentioned, various combinations of DCPA, TCPA, distance to the obstacle, speed, etc. are exploited in the literature to compute the risk index [4, 21-22]. This study proposes a new risk index based on ZMF functions (Section III). This index comprises the average of the DCPA, TCPA and distance to the obstacle as follows:

$$Risk(t) = (ZMF(|DCPA(t), a_{DCPA}, b_{DCPA}|) + |ZMF(TCPA(t), a_{TCPA}, b_{TCPA})| + ZMF(R(t), a_R, b_R)) / 3 \quad (29)$$

There are some advantages to this technique. Firstly, it normalizes the risk by mapping different distance and time

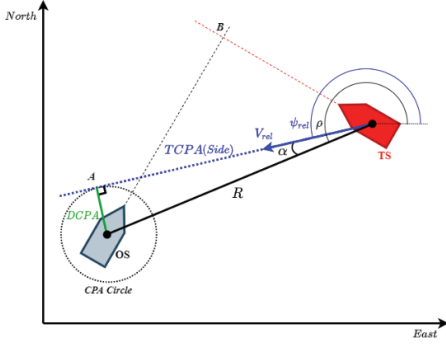


Fig. 3. Illustration of Closest Point of Approach (CPA) circle, and the right triangle with DCPA and TCPA sides

units between 0 to 1 which can be conveniently manipulated by simple algebra. Secondly, this index deploys the smooth ZMF function and enables the option to select two minimum and maximum risk levels for each sub-index. Finally, the outcome is a number between [0,1] which can be related to 0-100% of risk levels. As an instance, in this paper, four standard colours (green, yellow, amber, red) are used for indicating the different levels of risk. It should be noted other parameters such as relative velocity could be considered as sub-indexes of the risk. Nevertheless, using the ZMF functions is a contribution of this paper to compute the risk index.

B. COLLISION REGULATIONS (COLREGs)

When two vessels approach each other at sea, standard actions need to be taken as defined by COLREGs, the collision regulations outlined by the International Maritime Organisation [28]. Based on the COLREGs, once a TS is identified as a risk, three fundamental “head-on”, “crossing”, and “overtaking” situations are considered. An outcome of those situations could either be a “give-way” or “stand-on” action. In the “give-way” action, manoeuvre to the starboard or the port can be selected based on the scenario. Further details of the regulations can be found in [2, 11, 14, 28], however, the description of them is out of the scope of this paper. The general idea to classify the COLREGs variants is shown in Fig. 4. Moreover, to apply the required action in the planner, the corresponding value of K_{Dir} in (22) should be selected. In this paper, the starboard manoeuvre is the preferred course of action. This decision making is incorporated in the motion planning to behave based on the COLREGs rules.

In the next section, simulation results for the proposed algorithm are discussed.

V. SIMULATION RESULTS

In this section, simulation results for the proposed algorithm are presented. Three testing scenarios are considered. In the first scenario, a crossing (give-way) situation and a static obstacle are handled. The second and third tests explore overtaking and head-on scenarios, respectively. In all scenarios, the own vessel is assumed to be moving at a constant cruising speed of 16 m/s (32 knots). The model parameters are set to: $T_\psi = 30$, $K_\psi = 0.01$, $T_v = 50$, $K_v = 1$, $T_b = 600$. For $\omega_d(t)$ a white noise with a standard deviation of 0.5 is taken into account. An input amplitude saturation of ± 20 units is considered which alongside the dynamics of the vessel emulates the minimum turning radius of 80 m. The planning parameters are set to $D_m = 200$ m, $\mu =$

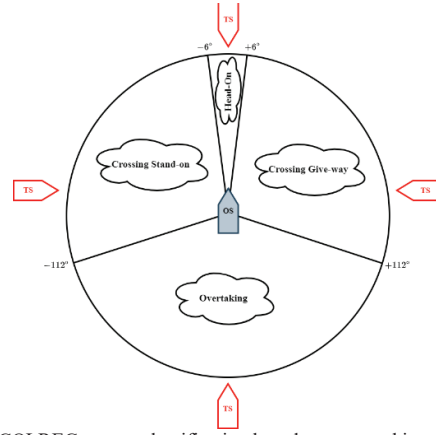


Fig. 4. COLREGs zones classification based on approaching vessel (OS: Own Ship, TS: Target Ship), for instance is the angle of approach between $\pm 6^\circ$ it is identified as heading-on

500, $\sigma = 80^\circ$, $K_{COLAV} = 2.0$, $a_{DCPA} = a_R = 300$ m, $b_{DCPA} = b_R = 1000$ m, $a_{TCPA} = 60$ s, and $b_{TCPA} = 240$ s.

A. Scenario I: Crossing Give-Way and a Static Obstacle

In this test, the OS encounters a crossing TS and a large obstacle during path following. OS is tracking waypoints initially in the northeast direction followed by a waypoint towards the east. The TS traverses with a speed of 9.5 m/s (18 knots) from the starboard side of the OS. A collision will be inevitable in case of no action by the OS. Based on COLREGs Rule 15, OS shall keep out of the way of the crossing vessel. A completed simulation analysis of this scenario is shown in Fig. 5. It should be noted, in all figures, the ship dimensions are scaled for better illustration and in no way reflect their actual size. Based on this Fig. 5, the OS has correctly altered its path towards the starboard to avoid the collision with the crossing vessel. Furthermore, the path correction is large enough to be visible by the target ship according to COLREGs rule 8. In addition, the target ship is illustrated by its associated risk colour in each sample. The COLAV performance in keeping away from the large static obstacle is also promising as depicted in Fig. 5.

In Fig. 6, time histories of the DCPA, distance to the obstacle $R(t)$, the TCPA and the risk parameter for the moving vessel are depicted. At the start of the simulation, the DCPA

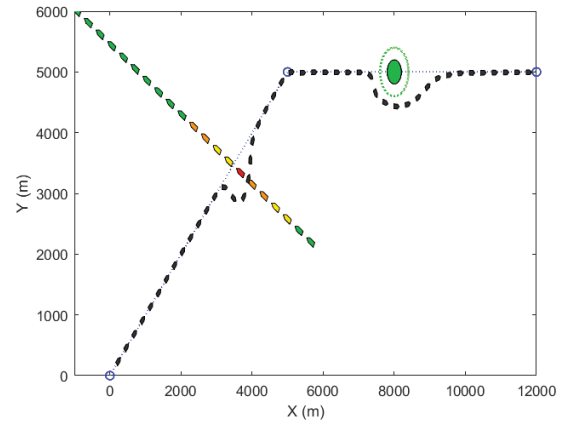


Fig. 5. Overall result of scenario I, give way to a crossing vessel from the starboard and a static COLAV (own vessel- Black, waypoints and the path- Blue, target vessel and the obstacles are coloured)

shows a value of zero representing a collision risk, however the TCPA was not small enough to take any action. Once in closer proximity, the action of the planner to alter the path results in the collision being avoided, and the vessel keeps a minimum distance of 450 m. The risk indicator signal in Fig. 6 also correctly identifies the risk when the distance between both vessels is the minimum where COLAV action occurs.

Fig. 7, exhibits the yaw command and its tracking as well as the control input. This figure demonstrates how the guidance and control systems work together to carry out the path following and avoidance manoeuvre demands.

B. Scenario II: Overtaking from Starboard

In the second scenario, an overtaking case is investigated. During the path following, the own vessel confronts another vessel moving at 6 m/s (12 knots) on the path ahead. Therefore, an overtaking action by keeping out of the overtaken vessel's way is necessary (based on Rule 13 of COLREGs). The simulation result in Fig. 8 demonstrates that the COLAV algorithm has successfully steered to overtake by keeping out of the way of the target ship. Since the scene is open water, a manoeuvre to starboard is selected.

Fig. 9, represents the DCPA, distance to the obstacle, the TCPA and the associated risk for the second scenario. Again, the DCPA and TCPA envisage the possibility of a collision before the 400th second, when the vessel starts the evasive manoeuvre. Variation of DCPA around zero before $t = 400$ s is because of the disturbances and their effect on the velocity

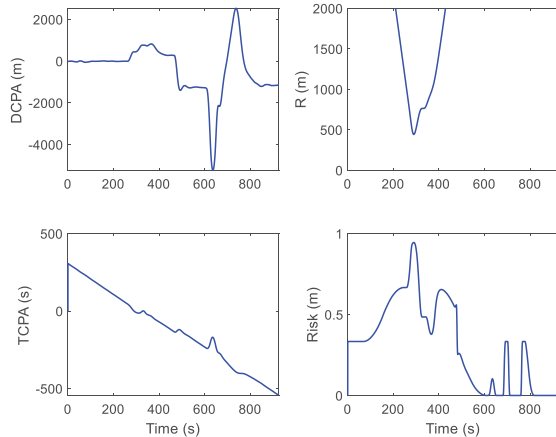


Fig. 6. DCPA, TCPA, Distance to the target ship (R) and Risk for the first simulation scenario

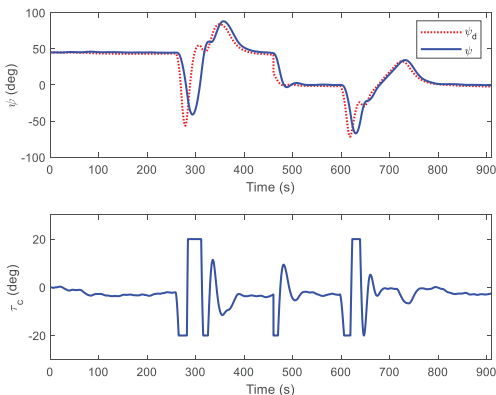


Fig. 7. Demanded and actual yaw (top) and the control signal (bottom) for scenario I

vector of the vessel. A minimum distance to collision of 580 m and lower risk are observed in this scenario compared to that of the previous one.

The yaw tracking performance and the control signal are shown in Fig. 10 which illustrates the feasible demand of the planner. Furthermore, large enough course alterations in yaw angle would cause higher visibility of the manoeuvre for the target ship according to COLREGs rule 8.

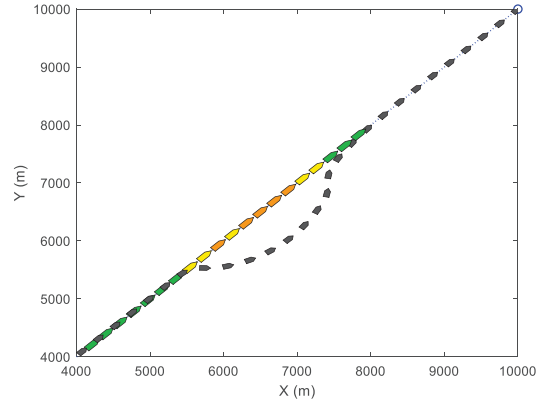


Fig. 8. Overtaking with keeping out of the way in scenario II (own vessel-Black, waypoints and the path-Blue, target vessel is coloured)

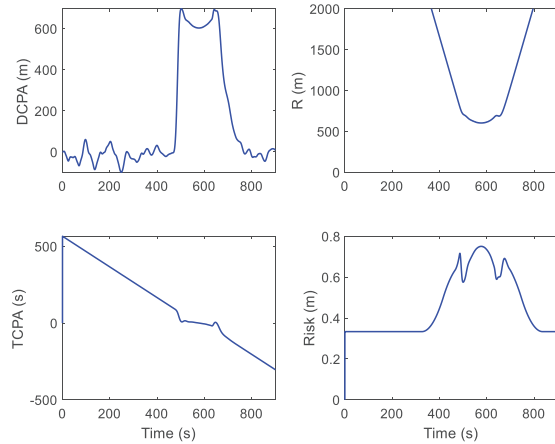


Fig. 9. DCPA, TCPA, Distance to the target ship (R) and Risk for the first simulation scenario

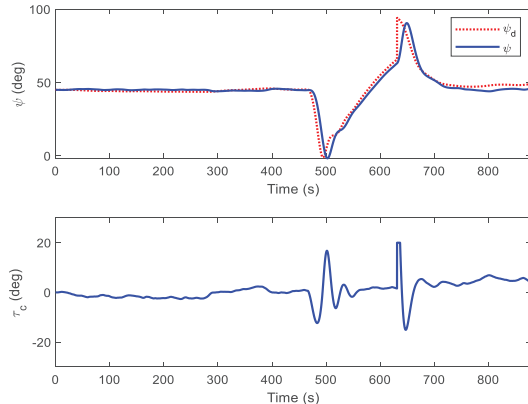


Fig. 10. Demanded and actual yaw (top) and the control signal (bottom) for scenario II

C. Scenario III: Head on

The third scenario considers the Head-on case. The own vessel is following a path to the northwest and a vessel approaching on an almost reciprocal course close to the planned path. Based on COLREGs Rule 14, both vessels shall change the course to the starboard to pass on the port side of each other. The results are shown in Fig. 11. The target ship moves at a speed of 9 m/s (18 knots) and it is assumed she does not alter her course. However, the own vessel activates the COLAV mode and modifies the path to eliminate any risk of collision. Fig. 12, illustrates the associated DCPA, TCPA, and

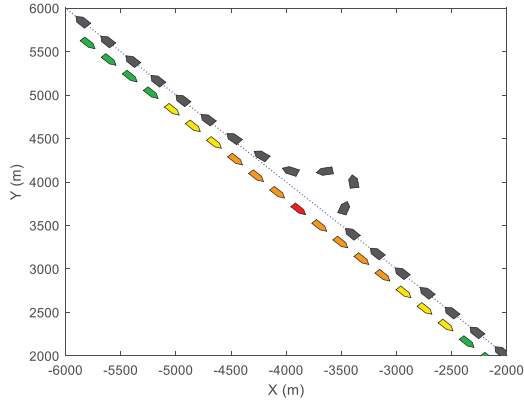


Fig. 11. Animation of the third scenario (Heading on), (own vessel- Black, waypoints and the path-Blue, target vessel is coloured)

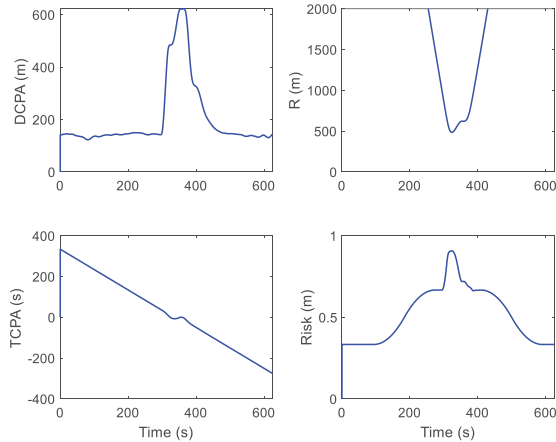


Fig. 12. DCPA, TCPA, distance and the risk to the target ship for the third scenario

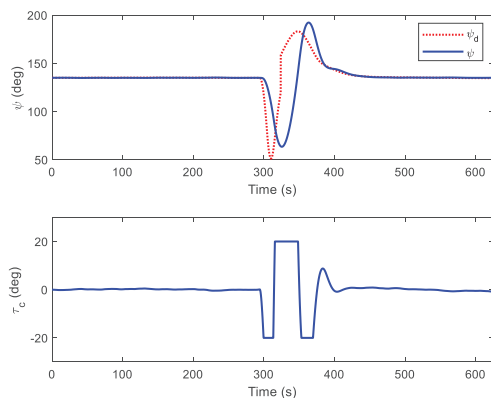


Fig. 13. Desired and actual yaw (top) and the control signal (bottom) for scenario III

distance and the risk to the target ship. It can be observed from this figure, once the risk increases, the own ship alters the path to decrease the risk and keeps a minimum distance of 480 m to the TS.

The yaw command tracking and the control signal for the third scenario are depicted in Fig. 13. Similar to the previous case, it can be observed that the demanded steering is feasible.

VI. CONCLUSION

In this study, preliminary results of Collision Avoidance (COLAV) and risk assessment techniques simulated on an autonomous catamaran were presented. While the method considers the main constraints and disturbances of the system, it is simple from an implementation point of view. Proposing a novel risk index and incorporating the COLREGs with this algorithm were some of the key contributions of this research. The method was simulated in typical collision encounter scenarios, and the obtained results were found to be promising. In the future, significant improvements can be considered such as generalization to restricted water scenarios, direct application of risk assessment in the COLAV algorithm and utilising the calculated risk index in machine learning techniques.

ACKNOWLEDGEMENT

The authors would like to thank the UK Research and Innovation for funding this project which is part of the Belfast Maritime Consortium under the Strength in Places Funding programme.

REFERENCES

- [1] S. Campbell, W. Naeem, and G. W. Irwin, "A review on improving the autonomy of unmanned surface vehicles through intelligent collision avoidance manoeuvres," *Annu. Rev. Control*, vol. 36, no. 2, pp. 267–283, 2012.
- [2] A. Vagale, R. Ouicheikh, R. T. Rye, O. L. Osen, and T. I. Fossen, "Path planning and collision avoidance for autonomous surface vehicles I: a review," *Journal of Marine Science and Technology*, Vol: 26, pp. 1292–1306, Jan. 2021.
- [3] A. Vagale, R. Ouicheikh, R. T. Rye, O. L. Osen, and T. I. Fossen, "Path planning and collision avoidance for autonomous surface vehicles II: a comparative study of algorithms," *Journal of Marine Science and Technology*, Vol: 26, pp. 1307–1323, Feb. 2021.
- [4] Y. Huang, L. Chen, P. Chen, R. R. Negenborn, and P. van Gelder, "Ship collision avoidance methods: State-of-the-art," *Safety Science*, vol: 121, pp. 451–473, Jan. 2020.
- [5] ---, "Yara to start operating the world's first fully emission-free container ship", <https://www.yara.com/corporate-releases/yara-to-start-operating-the-worlds-first-fully-emission-free-container-ship/>, visited in November 2021.
- [6] ---, "Artemis Technologies to build zero emissions ferries following £60M funding", <https://www.artemistechnologies.co.uk/artemis-technologies-to-build-zero-emissions-ferries-following-60m-funding/>, visited in November 2021.
- [7] ---, "Uncrewed Surface Vessel (USV) Cetus for marine data gathering and systems development", <https://www.plymouth.ac.uk/research/esif-funded-projects/usv-cetus>, visited in November 2021.
- [8] ---, "L3HARRIS technologies to design long-endurance autonomous surface ship concept for us defense advanced research projects agency", <https://www.l3harris.com/newsroom/press-release/2021/03/l3harris-technologies-design-long-endurance-autonomous-surface-ship>, visited in November 2021.
- [9] ---, "MAXCMAS success suggests COLREGs remain relevant for autonomous ships", <https://www.rolls-royce.com/media/press-releases/2018/21-03-2018-maxcmas-success-suggests-colregs-remain-relevant-for-autonomous-ships.aspx>, visited in November 2021.

- [10] Y. Kuwata, M. T. Wolf, D. Zarzhitsky, and T. L. Huntsberger, "Safe maritime autonomous navigation with COLREGS, using velocity obstacles," *IEEE Journal of Oceanic Engineering*, vol. 39, no. 1, pp. 110–119, Jan. 2014.
- [11] T. A. Johansen, T. Perez, and A. Cristofaro, "Ship collision avoidance and COLREGS compliance using simulation-based control behavior selection with predictive hazard assessment," *IEEE Tran. Intell. Transp. Syst.*, vol. 17, no. 12, pp. 3407–3422, Dec. 2016.
- [12] A. Lazarowska, "A discrete artificial potential field for ship trajectory planning," *J. Navigat.*, vol. 73, no. 1, pp. 233–251, Jan. 2020.
- [13] H. Lyu and Y. Yin, "COLREGS-constrained real-time path planning for autonomous ships using modified artificial potential fields," *J. Navigat.*, vol. 72, no. 3, pp. 588–608, May 2019.
- [14] L. Hu et al., "A multiobjective optimization approach for COLREGS compliant path planning of autonomous surface vehicles verified on networked bridge simulators," *IEEE Trans. Intell. Transp. Syst.*, vol. 21, no. 3, pp. 1167–1179, Mar. 2020.
- [15] H. Yamin, and P. H. A. J. M. van Gelder "Collision risk measure for triggering evasive actions of maritime autonomous surface ships," *Safety Science*, vol. 127, pp. 104708, Jul. 2020.
- [16] Z. Qiao, Y. Zhang and S. Wang, "A Collision Risk Identification Method for Autonomous Ships Based on Field Theory," in *IEEE Access*, vol. 9, pp. 30539-30550, 2021.
- [17] D. Kufalor et al., "Autonomous maritime collision avoidance: Field verification of autonomous surface vehicle behavior in challenging scenarios," *J. Field. Robot.*, vol. 37, no. 3, pp. 387-403, April. 2020.
- [18] L. Du, O. A. Valdez Banda, F. Goerlandt, Y. Huang, and P. Kujala,, "A COLREG-compliant ship collision alert system for stand-on vessels," *Ocean Engineering*, vol. 218, pp. 107866, Dec. 2020.
- [19] T. I. Fossen, *Handbook of marine craft hydrodynamics and motion control*. Belmont, John Wiley & Sons, 2011
- [20] A. J. Healey, "Guidance laws, obstacle avoidance and artificial potential functions," in *IEE Control Engineering Series*, G. N. Roberts, R. Sutton, The Institute of Engineering and Technology, London, United Kingdom, 2006, pp. 43–66.
- [21] Y. Huang and P. H. van Gelder, "Collision risk measure for triggering evasive actions of maritime autonomous surface ships," *Safety Science*, vol. 127, p. 104708, 2020.
- [22] P. Chen, Y. Huang, J. Mou, and P. H. van Gelder, "Probabilistic risk analysis for ship-ship collision: Stateof-the-art," *Safety Science*, vol. 117, pp. 108–122, 2019.
- [23] B. Li, and F. W. Pang, "An approach of vessel collision risk assessment based on the D–S evidence theory," *Ocean Engineering*, vol. 74, no. 7, pp. 16-21, Dec. 2013
- [24] H. Namgung and J. -S. Kim, "Collision Risk Inference System for Maritime Autonomous Surface Ships Using COLREGs Rules Compliant Collision Avoidance," in *IEEE Access*, vol. 9, pp. 7823-7835, 2021.
- [25] A. S. Lenart, "Analysis of collision threat parameters and criteria," *J. Navigat.*, vol. 68, no. 5, pp. 887–896, Sep. 2015.
- [26] S. Fossen, R. T. Bye and O. L. Osen, "Visualization and Collision Risk Assessment of Real Ships in a Mixed-Reality Environment using Live Automatic Identification System (AIS) Data," 2019 2nd European Conference on Electrical Engineering and Computer Science (EECS), 2018, pp. 217-223.
- [27] Captain Bob, "Collision Avoidance Radar Plotting 1," Radar Plotting Course, Northeast Maritime Institute, visited in November 2021, <https://www.youtube.com/watch?v=plunSIYEbUc>.
- [28] A. N. Cockcroft and J. N. F. Lameijer, *A Guide to the Collision Avoidance Rules*. Oxford, U.K.: Butterworth-Heinemann, 2003.